2009 American Control Conference
Hyatt Regency Riverfront, St. Louis, MO, USA
June 10-12, 2009

Cure-Feature Based Online Trajectory Generation in a Robotic Paint Curing System

Fan Zeng, Beshah Ayalew, and Mohammed A. Omar

Abstract—**Ultra-violate (UV) radiation-based robotic paint curing systems have great potential in improving energy efficiency and reducing the operating cost of the traditional oven-based units currently used in the automotive industry. This paper presents and compares two strategies for online trajectory generation in the control of such a robotic paint curing system. The system proposed here incorporates thermal vision feedback from an infra-red (IR) camera to ensure cure quality in the face of changing surface geometries and irradiance characteristics. To compare the two proposed strategies a computer simulation of the robotic curing system is developed. The results indicate that both strategies give comparable cure quality in the face of uneven target characteristics.**

I. Introduction

Traditionally, the process of automotive paint curing involved the use of convection ovens in assembly plants. Recently, some new radiation-based technologies, such as the ultra-violet (UV) curing, have been proposed and demonstrated as the better way to achieve equivalent curing performance with less working time and higher energy efficiency [1- 4]. This new methods are often integrated in a robotic curing system, which typically adds a UV lamp system to the end effector of an industrial manipulator. Often, these robotic UV curing systems are conceived to work in an open-loop 'sweep' manner, where the UV unit is swept across the target surface.

However, the highly complex surfaces of automobile bodies present challenges to such robotic UV curing systems due to the difficulties of fulfilling the required cure uniformity by sweeping the target with a small UV lamp attached on the end effector of the manipulator. To make this method practical for mass production, much calibrating work should be done to design an optimal path program for the manipulator and obtain satisfactory cure uniformity. This will increase the time and cost of the overall process. In addition, this calibration process may have to be repeated often since curing uniformity is influenced by the body styles and materials of car bodies.

Fan Zeng is with the Clemson University-International Center for Automotive Research, Greenville, SC 29607, USA (phone: 864-508-0998; fax: 864-283-7208; e-mail: fzeng@clemson.edu).

Beshah Ayalew is with the Clemson University-International Center for Automotive Research, Greenville, SC 29607, USA (email: beshah@clemson.edu).

Mohammed Omar is with the Clemson University-International Center for Automotive Research, Greenville, SC 29607, USA (email: momar@clemson.edu).

To simplify the above calibrating process and at the same time improve cure uniformity, some vision feedback control methods can be incorporated into the robotic UV curing system, such as adding a thermal signature feedback loop to monitor the online curing level [3]. A lot of research work has been done on the vision feedback control of a manipulator. Most of the approaches can be considered as a combination of both vision process routine and motion control routine [5]. Since the motion of the manipulator will greatly influence the irradiation of the target surface, the vision and control routines should be properly integrated. In general, a look-and-move method is preferred, which means the manipulator's action (i.e., orientation of the UV source) should be determined by both the motion controller and the feedback information which indicates the current curing level.

In this paper, two online trajectory generation strategies are developed, both of which use the cure features of the thermal images obtained by an infra-red (IR) camera incorporated in the system. An inverse dynamic algorithm is implemented to control the manipulator. Computer simulation models of the robotic curing process are used to evaluate the proposed strategies.

The rest of this paper is organized as follows. Section II describes the configuration of the robotic UV curing system and a simple model of the irradiation process. In Section III, two cure-feature based trajectory planning strategies are presented. The associated inverse dynamic control algorithm is discussed in Section IV. Section V gives the corresponding simulation results. Section VI presents the conclusion of this work.

II. System Configuration and Modeling

A. System Configuration

The proposed robotic UV curing system with thermal vision feedback is constituted by two basic routines in a serial manner: the vision process loop and the motion control loop, both of which are shown in Fig. 1. When the system starts to execute the curing process, it follows a two-step action, the first of which is to obtain the current thermal image of the target surface, extract the associated cure features and compare them with the desired ones. Then, suitable strategies are applied to generate the corresponding reference trajectory for the motion controller based on the cure features. The motion controller determines and applies the necessary torque

978-1-4244-4524-0/09/$25.00 ©2009 AACC

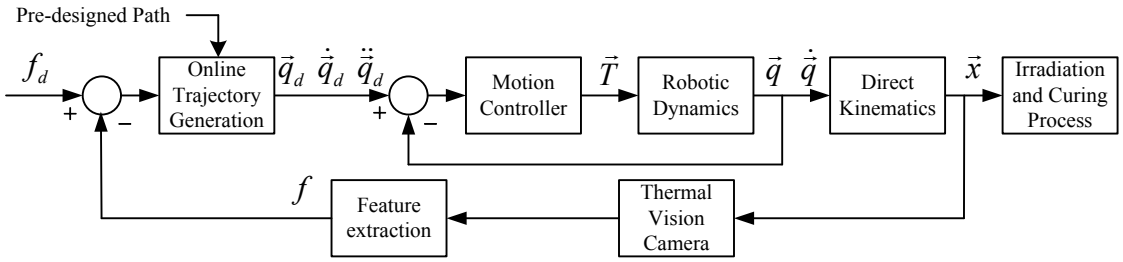

Fig. 1. The configuration of the robotic UV curing system with thermal vision feedback

to orient the manipulator with the UV lamp and cure the target surface properly.

In order to analyze this system, a mathematical model is developed to describe the robotic dynamics. In our work, we used the physical parameters of the PUMA560 manipulator [6], as we plan to conduct experiments with this particular manipulator. With the help of the encoders and potentiometers, the actual joint angles $\vec{q}$ and angular velocities $\dot{\vec{q}}$ can be measured to obtain the error for the controller to generate the driving torque $\vec{T}$. The direct kinematics block then calculates $\vec{x}$, the actual position and orientation of the end effector with the UV lamp. The current curing feature f is compared to the desired value f_d for online trajectory adjusting. To simulate the curing process, a simple irradiation model is established to describe the relationship between the curing status and the UV lamp configuration.

A. Modeling the Irradiation Process

The UV curing process is mainly influenced by the UV irradiation and the thermo-chemical reactions in UV sensitive paint pigments and other paint components. However, it is difficult to fully characterize both of them by using a simple control oriented model. If we assume the thermo-chemical reaction has been pre-specified for this application (i.e., pre-determined paint), and then the curing quality is primarily determined by the UV irradiation.

1) The source: Generally, two types of radiation sources are used in current UV curing technologies: the arc lamp with reflector and the LED array. The latter is rapidly developing and may become more suitable for automotive application due to its extremely long lifetime and instant on/off capability [1]. The UV LED array is usually composed of several cells, each of which can be simply characterized by an ideal Lambertian point source [7] shown in Fig. 2.

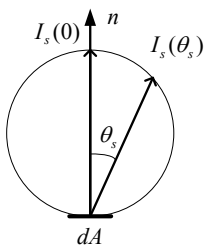

Fig. 2. The Lambertian point source

Fig. 2 describes the radiant intensity distribution of the Lambertian point source, which can be simply modeled as an ideal sphere with the following expression:

$$I_s(\theta_s) = I_s(0) \cdot \cos\theta_s = \frac{\phi}{\pi} \cdot \cos\theta_s \tag{1}$$

Here, ϕ is the radiant flux (W) of the source and θ_s represents the angle between the emissive direction and the normal direction of the source. The unit of the radiant intensity here is defined as the power per solid angle (W/sr).

2) The irradiation process: Since a radiation system is always composed of both a source and a receiver, the characteristics of the irradiation process are greatly influenced by their relative geometrical configuration [8]. Fig. 3 illustrates a typical radiative exchange between a source and a receiver unit.

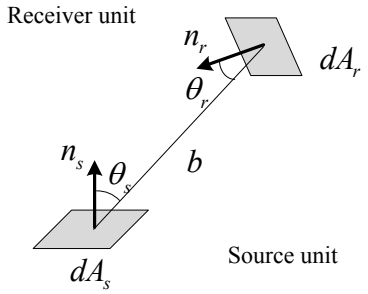

Fig. 3. The radiative exchange between a source and a receiver unit

In Fig.3, dA_s and dA_r denote the areas of the source and receiver units respectively. n_s and n_r are normal directions of the two units. θ_s and θ_r can be named as the emissive and receiving angles. According to the source model established in the previous subsection, the radiant intensity emitting at such direction can be obtained by using Eq.(1). However, the existence of the receiving angle indicates a partially absorption of the power from the source, which is defined as the irradiance E_r ($\mathrm{W/m^2}$):

$$E_r = k \cdot \frac{\phi \cdot \cos\theta_s \cdot \cos\theta_r}{\pi b^2} \tag{2}$$

Here, k is an efficiency factor which represents the absorbing characteristics of the receiver. From the view of the whole target surface, each receiver unit has its own value of k, which models the unevenness of the surface caused by the

painting process and/or surface geometry.

Since the UV LED array is constituted by several Lambertian-type source units, the total power radiated from the LED to the receiver unit can be obtained by superposition:

$$P(dA_r,t)=\int_{As} k\cdot\frac{\phi\cdot\cos\theta_s\cdot\cos\theta_r}{\pi b^2}dA_s \tag{3}$$

The corresponding absorbed energy is computed by integrating the power with respect to time:

$$E(dA_r,t)=\int_0^t P(dA_r,t)dt \tag{4}$$

It can be seen from the above expression that the absorbed energy of the receiver unit is a function of both the coordinate and the time, because the UV LED will move with the end effector during the curing process. At the same time, the geometrical configurations between the LED array and each receiver unit will change correspondingly. Calculating the absorbed energy for each unit at each time step, we can obtain the time-variant energy distribution of the target surface, which is considered to be proportional to the temperature distribution captured by the IR camera.

III. CURE-FEATURE BASED TRAJECTORY GENERATION

The main task of trajectory generation is to provide the reference input for the motion controller in operation space or joint space so that the manipulator can execute the desired work [9-10]. Most of the trajectory-planning processes for current industrial manipulators are done off-line by the programmer. However, the time-variant property of the UV curing process makes it difficult to achieve the desired uniformity through a fixed pre-designed trajectory due to the uncertainties of the target, such as the uneven surface, variant absorbing efficiency of the paint and so on. Therefore, we propose some online trajectory generation strategies based on the cure features extracted from the thermal image in order to compensate those uncertainties. Considering different locations of the IR camera, two trajectory generation strategies are presented below.

A. Local Camera Strategy

In this case, the IR camera is installed on the end effector of the manipulator and will be moved with the UV LED during the curing process. Since the end effector is usually very close to the target surface, the camera can cover only a small patch currently being cured by the UV LED at each time step. Therefore, the cure-feature provided by the camera now is the average energy distribution of the covered area. The local camera acquires a new image when the manipulator comes to a complete stop. Then the trajectory generation strategy in this situation can be described as a discrete-moving type strategy, including the following two steps:

1) The moving step: After the previous area has been cured, the manipulator begins to move the end effector to the next area along the pre-designed path in a fast and smooth manner with the UV LED and IR camera essentially turned off.

2) The curing step: When the end effector arrives at the new area, the UV LED starts to cure that area and the IR camera acquires the thermal image until the cure feature achieves the desired value. At this point, the manipulator executes another moving step. This trajectory generation strategy can be illustrated by Fig. 4 in the joint space.

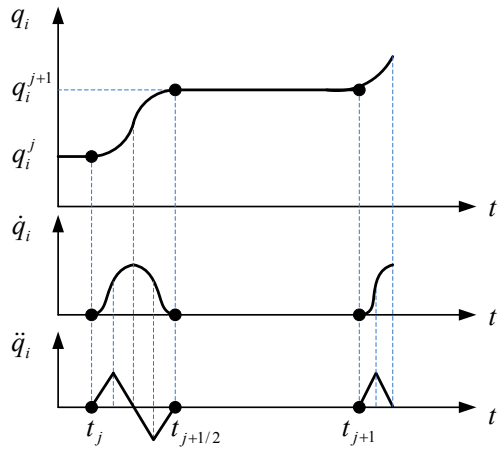

Fig. 4. Trajectory of joint position, velocity and acceleration

In Fig. 4, q_i denotes the position trajectory of the i^{th} joint of the manipulator. $\dot{q}_i$, $\ddot{q}_i$ represent the corresponding velocity and acceleration trajectories. The position trajectory describes a complete two-step cycle when the manipulator executes the curing process at one patch of the target surface. First, the end effector is moved from the previous area to the new one, and then the associated angle for the i^{th} joint will change from q_i^j to q_i^{j+1}. A spline type of trajectory is selected to smooth this movement. Then the manipulator will stop at the current area until the corresponding curing process is done. The duration of the moving and curing steps can be calculated by:

$$\Delta t_{moving}=t_{j+1/2}-t_j \tag{5}$$

$$\Delta t_{curing}=t_{j+1}-t_{j+1/2} \tag{6}$$

Since the UV LED and IR camera are off during the moving step, the duration Δt_{moving} can be pre-designed based on the dynamic characteristics of the manipulator. The curing duration Δt_{curing} will be determined online according to whether the desired curing level has been achieved with the help of the thermal vision feedback from the IR camera.

B. Global Camera Strategy

Compared with the local camera strategy, the global one will mount the IR camera on some stationary rack with an appropriate distance from the target surface in order to obtain a wide view. In this case, the camera can cover the whole target surface during the curing process. Then, two features can be extracted from such thermal image: the curing level and the associated coordinate. Based on these features, the global camera strategy can be design as a look-sweep type which

consists of the following two steps:

1) The pre-sweeping step: At this step, the manipulator will first sweep the whole target surface with a constant speed and then comes to a complete stop for the fixed camera to acquire the thermal image. Due to the uncertainties of the target surface, it may get an image which can be divided into sections with different curing levels. The curing level is defined as:

$$\text{curing level} = \frac{\text{current energy}}{\text{desired energy}}$$

Fig. 5 gives a distribution example after the UV LED horizontally sweeps a simple rectangular plane with different absorbing efficiency factors.

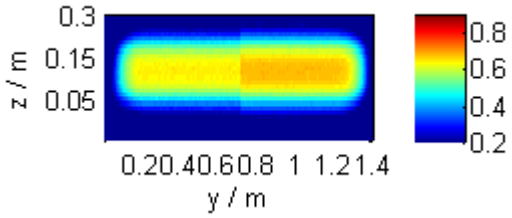

Fig. 5. Curing level distribution of a simple plane with different absorbing efficiency factors after the pre-sweeping step

It can be seen from Fig. 5 that along the path of the end effector, the right half has a higher curing level (about 0.75) than the left one (about 0.65). The y coordinate of the dividing line is around 0.7m. These features can be used to adjust the manipulator's motion in next step.

2) The adjusting step: After the camera obtains the current thermal feature of the target surface, the manipulator will sweep the surface again to adjust the curing level based on the status of the pre-sweeping step. At this time, the manipulator is supposed to increase the sweeping speed for both the left and right parts in Fig. 5, since they have already been pre-swept. Particularly, it should move faster when it crosses the dividing line in order to compensate the higher curing level at the right half. This adjusting process may be repeated by two or three times until the curing level distribution of the target surface achieves the desired value.

In this strategy, the corresponding trajectory generation should be done in the operational space, since the speed of the end effector will change online during the adjusting step. However, this requires the inverse kinematics to be taken online and this may increase the computational cost. To simplify that process, a path-point method can be applied to approximate the speed requirement in the operational space [10]. Fig. 6 illustrates the basic idea of this method, considering only the y coordinate of the end effector.

To complete a sweeping movement, it starts from the initial position y_i with zero velocity and then accelerates to a constant speed. When it is close to the final position y_f, it will decelerate to zero velocity and reach the destination. The path-point method will approximate the whole path by several

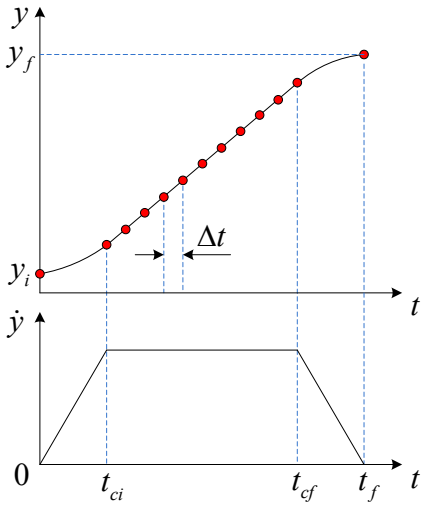

Fig. 6. Path-point method

points to describe the end effector's location in the operational space at given time instants. By solving the inverse kinematics, we can get the associated joint angle for each point off-line. The accelerating time t_{ci} and decelerating time $t_f - t_{cf}$ can also be pre-designed based on the dynamic property of the manipulator. Then, the sweeping speed will be determined by the duration Δt between two adjacent points during the constant-speed part. Therefore, to compensate the unevenness in Fig. 5, the trajectory generation of the adjusting step can be done by varying Δt as shown in Fig. 7.

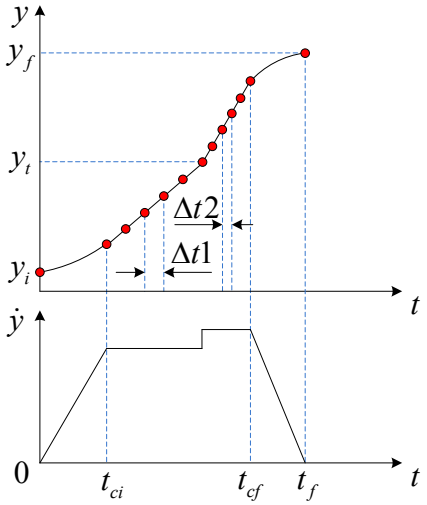

Fig. 7. Adjusted trajectory for compensating the unevenness in Fig. 5

In Fig. 7, when the manipulator sweeps the left half of the plane shown in Fig. 5, the duration between two adjacent points is set to $\Delta t1$. After it crosses the dividing line (y_t), the duration will be decreased to $\Delta t2$ in order to obtain a faster sweeping speed. Since the two strategies mentioned above only adjust the time law of the trajectory, the inverse kinematics can be done off-line and this reduces the computational cost and simplifies the whole process.

IV. MOTION CONTROL DESIGN

In this work, an inverse dynamic algorithm was used to control the 6DOF manipulator in the joint space. The governing equation of the manipulator can be represented by:

$$D(\vec{q})\ddot{\vec{q}} + C(\vec{q},\dot{\vec{q}})\dot{\vec{q}} + G(\vec{q}) = \vec{\tau} \quad (7)$$

In equation (7), $\vec{q}$ and $\dot{\vec{q}}$ represent the rotating angle and angular velocity of six joints respectively. The coefficient matrix $D(\vec{q})$ denotes the moment of inertia at each joint and the coupling inertias between joints. The matrix $C(\vec{q},\dot{\vec{q}})$ represents centrifugal and Coriolis effects. The vector $G(\vec{q})$ represents the moment generated at each joint by the presence of gravity. The model of the manipulator, which in our work was a PUMA 560, was established in a multi-body dynamics software called SIMPACK, using parameters identified by [6]. The control input is generated by using feedback linearization [11] as follows:

$$\vec{\tau} = C(\vec{q},\dot{\vec{q}})\dot{\vec{q}} + G(\vec{q}) + D(\vec{q})\vec{v} \quad (8)$$

$$\vec{v} = -K_V\dot{\vec{q}} - K_P\vec{q} + \left(\ddot{\vec{q}}_d + K_V\dot{\vec{q}}_d + K_P\vec{q}_d\right) \quad (9)$$

In equation (8), we calculate $C(\vec{q},\dot{\vec{q}})$, $G(\vec{q})$ and $D(\vec{q})$ based on the parameters and current configuration of the manipulator. Substituting (8) and (9) into (7), we can obtain the following linearized system:

$$\left(\ddot{\vec{q}}_d - \ddot{\vec{q}}\right) + K_V\left(\dot{\vec{q}}_d - \dot{\vec{q}}\right) + K_P\left(\vec{q}_d - \vec{q}\right) = 0 \quad (10)$$

or

$$\ddot{\vec{e}} + K_V\dot{\vec{e}} + K_P\vec{e} = 0 \quad (11)$$

Here, $\vec{q}_d$, $\dot{\vec{q}}_d$ and $\ddot{\vec{q}}_d$ represent the reference position, velocity and acceleration of the joints generated by the trajectory planning process. The coefficient matrices K_V and K_P were selected diagonally and optimally to achieve the desired control performance for each joint independently.

V. SIMULATION RESULTS

The model of the proposed robotic UV curing system was established as a co-simulation between MATLAB/Simulink and SIMPACK softwares. The two on-line trajectory generation strategies are implemented in the simulation and their performances are compared.

To demonstrate the ideas, we selected a simple rectangular plane as the target surface, the dimension of which is 1.4m× 0.3m. The unevenness caused by the inhomogeneous painting and unsmooth geometry can be characterized by two parameters: the efficiency factor k mentioned in section II and the distance d between the target surface and the UV LED panel. Here, we use two simple examples to illustrate the unevenness of the target surface, as shown in Fig. 8.

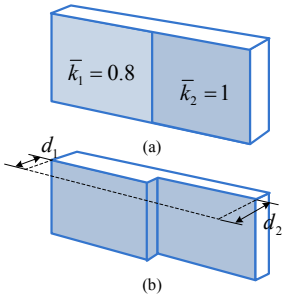

Fig. 8. (a) Unevenness caused by different efficiency factors (b) Unevenness caused by different geometric features

In Fig. 8(a), different efficiency factors are assigned to the left and right parts of the target surface respectively. Possible randomness in surface paint unevenness is modeled using a statistical distribution of the absorption efficiency. Therefore, the efficiency factors of the left part have a mean of $\bar{k}_1 = 0.8$ and a variance of 0.01. Similarly, those of the right part have a mean of $\bar{k}_2 = 1$ and a variance of 0.01. Fig. 8(b) depicts the unevenness caused by different geometrical features. The left and right parts have different distances (d_1, d_2) away from the path of the UV LED panel. In this case, d_1, d_2 are set as 0.03m and 0.04m respectively, and the efficiency factor of the whole target surface is simply assumed to be 1. A simple linear path is designed for the end effector to sweep the plane back and forth. Then, the whole plane is quantized into 140× 30 units and the absorbing energy of is calculated by using (4) to obtain the curing level distribution. The corresponding simulation results are shown in Figs. 9-12 in terms of color maps and cure level curves.

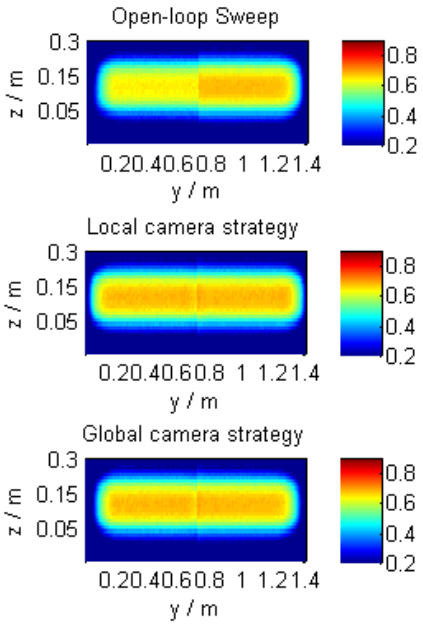

Fig. 9. Curing level distribution of the whole plane for Fig. 8 (a)

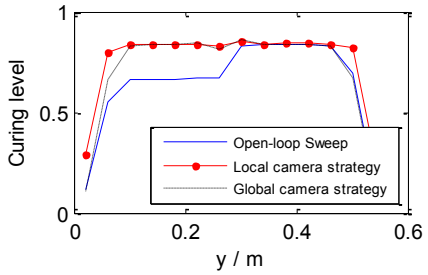

Fig. 10. Curing level distribution along the path for Fig. 8 (a)

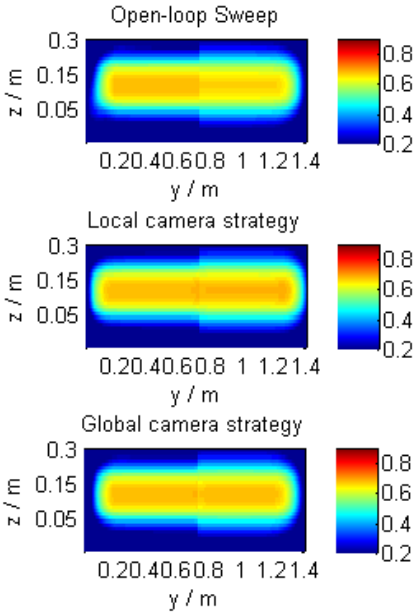

Fig. 11. Curing level distribution of the whole plane for Fig. 8 (b)

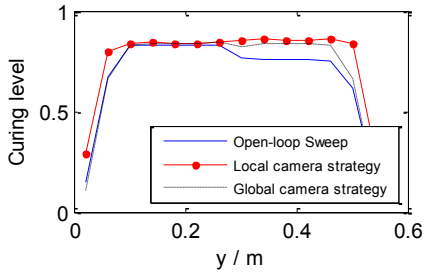

Fig. 12. Curing level distribution along the path for Fig. 8 (b)

Fig. 9 gives the curing level distribution of the whole plane with the unevenness defined as in Fig. 8(a). Fig. 10 illustrates the associated curing level distribution along the path. Both of them give the comparison among three different curing strategies, including the open-loop sweep and the two methods mentioned in Section III. The open-loop sweep follows the same path as those with the thermal vision feedback. The results show that both the local and global camera strategies achieve a good curing uniformity for this test case. Similarly, Figs. 11 and 12 give the curing level distribution for the example of Fig. 8(b). Although the result in Fig. 11 shows unevenness near the (transverse) sides due to the geometric step, the curing level distribution along the path in Fig. 12 still demonstrates that the two strategies can help improve the curing uniformity under the geometrical unevenness of the target.

VI. Conclusion

This paper presented an analysis of cure-feature based feedback control of a robotic UV curing system. Two online trajectory generation methods referred to as the local and global camera strategies are proposed and evaluated. These strategies adjust the UV manipulator trajectories based on the cure-feature feedback obtained from an IR camera. The simulation evaluation of the robotic cure system employing both the local and global camera strategies showed that they can succeed in compensating the unevenness caused by painting irregularities and/or geometry irregularities during the curing process.

The authors are pursuing an experimental implementation of these proposed closed loop curing strategies to verify the stated benefits of robotic UV curing in automotive manufacturing.

References

[1] Schwalm, R., "UV Coatings: Basic, Recent Developments and New Applications", Elsevier, Amesterdam, the Netherlands, 2007.

[2] Mills, P., "Robotic UV Curing for Automotive Exterior Applications: A cost-effective and technically viable alternative for UV curing", North American Automotive UV Consortium Report, Stongsville, OH, 2005.

[3] Zeng, F., Ayalew, B., and Omar, M., "Robotic Automotive Paint Curing Using Thermal Signature Feedback", Industrial Robot: An International Journal, 2008 (Accepted, in press)

[4] Thomas Raith, Markus Bischof, Michael Deger and Elisabeth Gemmler, "3-D UV Technology for OEM Coatings", RadTech Report Article on Robotic UV Curing at Daimler Chrysler, Germany, 2001.

[5] Feddema, J. T., Mitchell, O. R., "Vision-guided Servoing with Feature-based Trajectory Generation", IEEE Transactions on Robotics and Automation, vol. 5, no. 5, 1989, pp. 691-700.

[6] Corke, P. I., Armstrong-Helouvry, B., "A Search for Consensus among Model Parameters Reported for the PUMA 560 Robot", IEEE International Conference on Robotics and Automation, vol. 2, 1994, pp. 1608-1613.

[7] Ashdown, I., "Radiosity: A Programmer's Perspective", John Wiley and Sons, New York, NY, 1994.

[8] Modest, M. F., "Radiative Heat Transfer", McGraw Hill, New York, NY, 1993.

[9] Paul, R. P., "Robot Manipulators: Mathematics, Programming, and Control", MIT Press, Cambridge, MA, 1982.

[10] Sciavicco, L., and Siciliano, B., "Modeling and Control of Robot Manipulators", Springer, London, UK.

[11] Slotine, J. J. and Li, W., "Applied Nonlinear Control", Prentice Hall, NJ, 1991.